Acoustic characteristics of forage fish species in the Gulf of Alaska and Bering Sea based on Kirchhoff-approximation models

Stéphane Gauthier and John K. Horne

Abstract: Acoustic surveys are routinely used to assess fish abundance. To ensure accurate population estimates, the characteristics of echoes from constituent species must be quantified. Kirchhoff-ray mode (KRM) backscatter models were used to quantify acoustic characteristics of Bering Sea and Gulf of Alaska pelagic fish species: capelin (*Mallotus villosus*), Pacific herring (*Clupea pallasii*), walleye pollock (*Theragra chalcogramma*), Atka mackerel (*Pleurogrammus monopterygius*), and eulachon (*Thaleichthys pacificus*). Atka mackerel and eulachon do not have swimbladders. Acoustic backscatter was estimated as a function of insonifying frequency, fish length, and body orientation relative to the incident wave front. Backscatter intensity and variance estimates were compared to examine the potential to discriminate among species. Based on relative intensity differences, species could be separated in two major groups: fish with gas-filled swimbladders and fish without swimbladders. The effects of length and tilt angle on echo intensity depended on frequency. Variability in target strength (TS) resulting from morphometric differences was high for species without swimbladders. Based on our model predictions, a series of TS to length equations were developed for each species at the common frequencies used by fisheries acousticians.

Résumé : Les inventaires acoustiques sont utilisés régulièrement pour estimer l'abondance des poissons. Pour obtenir des estimations précises, les caractéristiques des échos provenant des différentes espèces doivent être quantifiées. Des modèles de réflexion acoustique fondées sur l'approximation de Kirchhoff ont été utilisés pour mesurer les propriétés acoustiques de plusieurs espèces dans le Golf de l'Alaska et la Mer de Béring : le capelan (*Mallotus villosus*), le hareng du Pacifique (*Clupea pallasii*), la goberge de l'Alaska (*Theragra chalcogramma*), le maquereau Atka (*Pleurogrammus monopterygius*) et l'eulakane (*Thaleichthys pacificus*). Le maquereau Atka et l'eulakane n'ont pas de vessies natatoires. La rétro-diffusion acoustique a été estimée en fonction de la fréquence sonore, de la taille et de l'orientation des poissons. L'intensité des échos et leur variance ont été comparées pour examiner la possibilité de discerner les espèces. Nous avons découvert que les espèces peuvent être séparées en deux groupes selon la présence ou l'absence de vessie natatoire. L'incidence de la taille et de l'orientation sur l'intensité des échos dépendaient de la fréquence sonore. La variabilité de l'indice de réflexion (IR) due aux différences morphométriques était élevée pour les espèces sans vessie. Des équations mettant en rapport la taille des poissons et l'IR ont été élaborées pour chaque espèce en fonction des fréquences sonores les plus couramment utilisées.

Introduction

Acoustic surveys are used to monitor the distribution, abundance, and habitat use of fish within ecosystems. These surveys are appealing for assessment purposes as large volumes of water are rapidly sampled at high spatial and temporal resolutions. To convert acoustic signals to estimates of fish abundance, species must be properly partitioned within survey areas and the echo energy of constituent species must be known. The intensity of an echo is generally expressed on a logarithmic scale as the target strength (TS). Acoustic properties of fish are species-specific and change over time. In addition to physical characteristics such as frequency (Foote 1982), TS depends on fish size (Nakken and Olsen 1977), anatomical features (e.g., presence of a swimbladder; Foote 1980*a*), morphology (e.g., swimbladder shape; McClatchie et al. 1996*a*), and physiological state (e.g., gonadal maturation and gut fullness; Ona 1990). Fish behavior can also significantly alter TS through changes in fish orientation relative to the wave front (Nakken and Olsen 1977; Foote 1980*b*; Blaxter and Blatty 1990) and vertical movement within the water column, which changes swimbladder volume (Ona 1990; Mukai and Iida 1996; Rose and Porter 1996). Ideally, TS should be measured under the same conditions as those encountered when populations are surveyed. Suitable in situ conditions for the measurement of TS can be difficult to ob-

Received 2 October 2003. Accepted 16 April 2004. Published on the NRC Research Press Web site at http://cjfas.nrc.ca on 11 December 2004.
J17772

S. Gauthier[1] and J.K. Horne. University of Washington, School of Aquatic and Fishery Sciences, Box 355020, Seattle, WA 98195-5020, USA.

[1]Corresponding author (e-mail: sgau@u.washington.edu).

 doi: 10.1139/F04-117

tain, especially in mixed species aggregations or within dense schools of fish.

A modeling approach provides a practical alternative to measurements and can be used to examine the amplitude and variability of acoustic backscatter as a function of single or multiple variables. Modeling exercises can also be used to compare and contrast acoustic properties among species and identify potential metrics for species discrimination and identification. The Kirchhoff-ray mode (KRM) model uses low-mode solutions and Kirchhoff-ray approximations to estimate resonant and geometric backscatter using planar images of the fish body and swimbladder (Clay and Horne 1994). KRM model predictions have been successfully matched to empirical measures (Jech et al. 1995; Horne et al. 2000; Horne 2003). Matches of KRM model predictions to empirical backscatter measurements of pollack (*Pollachius pollachius*) and saithe (*Pollachius virens*) were comparable to those obtained using the boundary element model (BEM) over a frequency range of 38.1 to 120.4 kHz (Foote and Francis 2002). In the present study, KRM models are used to characterize acoustic properties of forage fish in the Gulf of Alaska and the Bering Sea. Five abundant and widely distributed species are considered: capelin (*Mallotus villosus*), Pacific herring (*Clupea pallasii*), walleye pollock (*Theragra chalcogramma*), Atka mackerel (*Pleurogrammus monopterygius*), and eulachon (*Thaleichthys pacificus*). Atka mackerel and eulachon do not possess swimbladders. Capelin and Pacific herring are physostomous (open swimbladder), whereas walleye pollock is physoclistous (closed swimbladder).

These fish species are important to the diet of many apex predators such as Steller sea lions (*Eumetopias jubatus*). Recent declines in western Steller sea lion populations in the Gulf of Alaska and the Bering Sea have increased interest in the assessment of forage fish species (Alverson 1992). It has been hypothesized that changes in the composition, distribution, and availability of fish in Steller sea lion habitat are in part responsible for their decline and lack of recovery (Rosen and Trites 2000; Stickney 2000; Trites and Donnelly 2003). Some of the challenges associated with the acoustic assessment of forage fish around Steller sea lion rookeries, haulouts, and feeding grounds include accurate conversion of acoustic energy to fish biomass and species discrimination in mixed fish aggregations. Our work examines acoustic characteristics of these forage species and identifies possible steps in the ongoing effort to develop acoustic discrimination techniques.

Materials and methods

Radiographs and digital pictures were used to image fish bodies and swimbladders used in KRM modeling (Fig. 1). Fish were captured using hand lines or midwater trawls and were kept in aerated tanks. When possible, a period of at least 12 h was allowed for fish with swimbladders captured at depth to acclimate to surface pressure. Fish were subsequently anesthetized for a period of 30–60 s in a 10-L basin of water containing 5 mL of a 9:1 mixture of ethanol to clove oil. Once immobilized, fish were placed individually on a flat surface for lateral and dorsal imaging. Fish with a swimbladder were radiographed using a portable veterinary x-ray unit (XTEC Laseray 90P; XTEC Inc., Columbia City, Indiana). The fish were placed at a focal distance of 40–45 cm on cassettes or redipaks containing rare earth film. Fish lateral and dorsal planes were exposed at 15 mA for 2 s at 95 kVp on the redipaks (generally used for <25-cm fish) or for 0.18 s at 70 kVp on cassettes with intensifying screens (generally used for >25-cm fish). Fish without swimbladders were photographed using a 3.3-megapixel digital camera (photoPC 3000z; Epson America Inc., Long Beach, Calif.). Lateral and dorsal images of the fish body and swimbladder (when present) were traced on acetate sheets, scanned, and then digitized at 1-mm resolution. Fins and tail were not included in the trace. Orientation of the swimbladder relative to the body was maintained, and the body parts were scaled to their true size using maximum and minimum body and swimbladder measurements. When necessary, trace lines were smoothed and rotated so that the sagittal axis of the fish body was horizontal. The resulting dorsal and lateral images were elliptically interpolated into 1-mm-thick cylinders to give a three-dimensional (3D) representation of the fish body and swimbladder (Fig. 2). A series of morphometric descriptors (including swimbladder volume and area) were estimated using these 3D fish representations. Species were partitioned into groups of similar-sized individuals (10-cm length groups). The ratio of the major to minor axes of the body and swimbladder (maximum length and width) were measured on the lateral traces as an index of elongation. The eccentricity (e) of the fish body or swimbladder was also measured as the ratio of the distance between the foci and the vertices of an ellipse having the same major and minor axes as the fish trace. Eccentricity varies between 0 and 1 ($0 \le e < 1$, where 0 is a circle).

Swimbladders were modeled as a series of gas-filled cylinders, and fish bodies were modeled as a series of fluid-filled cylinders. The energy backscattered by the fish body and swimbladder was obtained by estimating the scattering from each cylinder (for details see Clay and Horne 1994). The scattered sound pressure (P_{scat} at time t and range R) of an object insonified by a plane incident wave (of amplitude P_{inc} at the object) is

$$(1) \qquad P_{scat}(t,R) = (P_{inc}/R)\, e^{i(kR-2\pi ft)} \mathcal{L}(t)$$

where k is the wave number (m^{-1}), f is the frequency (Hz) for the convolution of the sound wave, and $\mathcal{L}(t)$ is the scattering length (m) of the object in the time domain. Scattering amplitudes from the fish body and swimbladder were added coherently to obtain the total scattering length of the fish. The absolute square of the scattering length is equivalent to the backscattering cross section of an insonified object (σ_{bs}, m^2):

$$(2) \qquad \sigma_{bs} = |\mathcal{L}|^2$$

where $\mathcal{L}$ is a function of the insonifying frequency and length (L, m) of the object. Our model combines these variables as a nondimensional reduced scattering length (RSL):

$$(3) \qquad \mathrm{RSL} = \mathcal{L}(L/\lambda)/L$$

where λ is the acoustic wavelength (m). RSLs obtained in the frequency domain can be converted to target strength (TS, dB) at any specified length:

$$(4) \qquad \mathrm{TS} = 20\log(\mathrm{RSL}) + 20\log(L)$$

Fig. 1. Illustrations of the modeled species with corresponding lateral and dorsal radiographs (traces shown for species that do not possess a swimbladder). The air-filled swimbladder can be seen as a dark shape within the fish body, and the different shades of gray represent structures of different densities within the fish body (lighter shade = densest, as a result of high x-ray absorption).

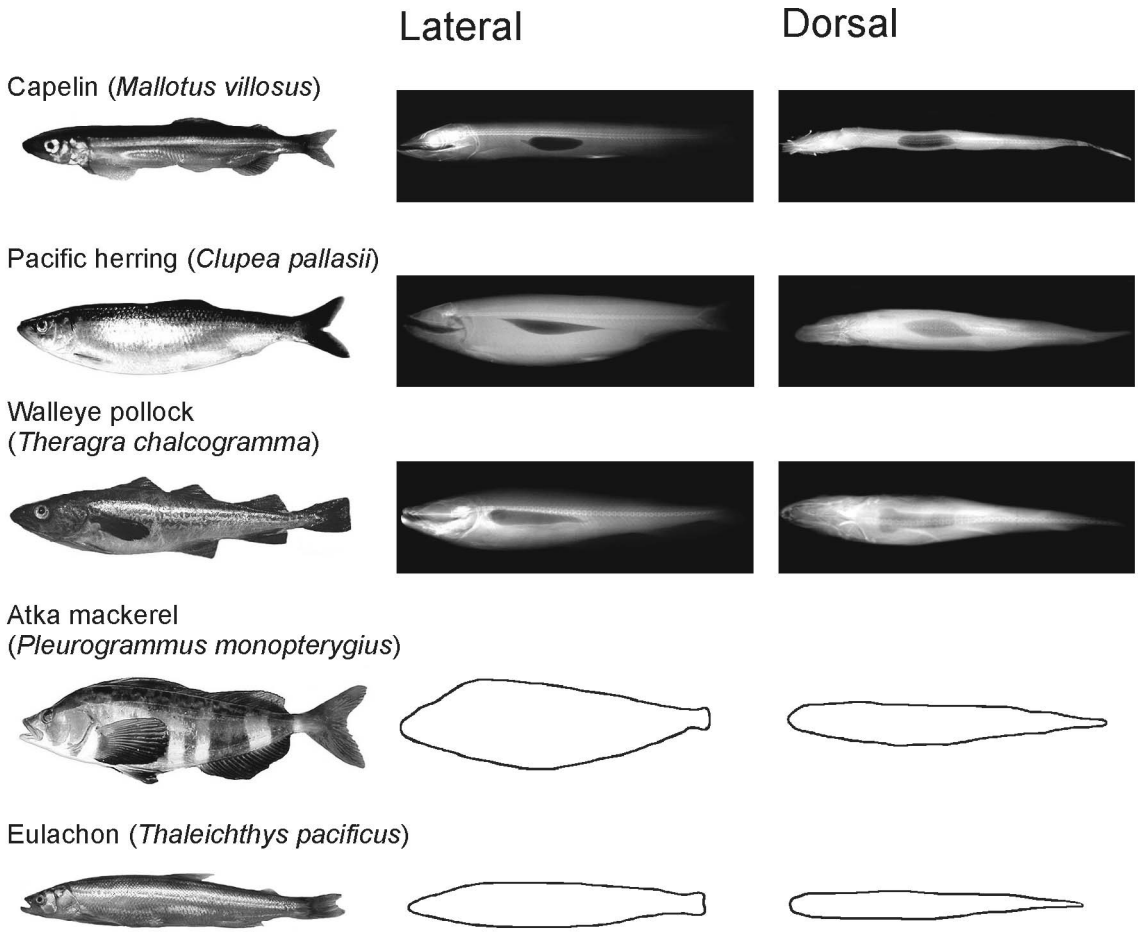

We list the parameters used in KRM modeling (Table 1). Eulachon (an anadromous species) was modeled for both marine and freshwater environments.

For each species, TS was estimated as a function of length, carrier frequency, and tilt angle. The effect of one variable (e.g., length) was modeled for each fish over an arbitrary range by controlling for the other factors (e.g., fixed frequency and tilt angle in this case). Predicted RSL values were compiled for all digitized fish to obtain a mean and standard deviation of the acoustic backscatter for each species and size group. When representing the average value for a group of individuals, TS was denoted as $\overline{\mathrm{TS}}$. To estimate backscatter over a common length range, fish were linearly scaled in each dimension to all lengths within the modeled range. Length ranges (at 2-mm increments) were centered on the average length of collected specimens. The effect of frequency was modeled from 12 to 420 kHz. Tilt angles were modeled at increments of 1° over a range of 45° to 135°, where 90° represents a normal aspect (i.e., lateral axis of the fish body perpendicular to the incident wave front). The effects of length and frequency were modeled at dorsal incidence (normal aspect). Frequency and tilt angle effects were modeled at various scaled fish lengths.

Model results were used to estimate tilt-averaged target strength (TS_θ) to total length (L_T) relationships for the five studied species. To estimate TS_θ, reduced scattering lengths (RSL) were generated for each individual at their actual length over a range of 45° to 135° at 1° increments. A normal distribution of tilt angles having a known mean and standard deviation (based on in situ measurements when available) was randomly sampled to provide 1000 tilt values (Table 2). Echo-intensity values were tabulated from this tilt-angle distribution and corresponding model predictions. The resulting TS_θ of individual fish were subsequently used to estimate the regression parameters for each of the five species. The models were generated as

$$\mathrm{TS}_\theta = a \log(L_\mathrm{T}\ (\mathrm{cm})) + b_a \quad (5)$$

$$\mathrm{TS}_\theta = 20 \log(L_\mathrm{T}\ (\mathrm{cm})) + b_{20} \quad (6)$$

where a is the slope and b_a (or b_{20}) is the intercept of the regression. The regression parameters were calculated at the five frequencies most commonly used in fisheries acoustics (12, 38, 70, 120, and 200 kHz). KRM predicts TS using fish caudal lengths (length from tip of snout to end of caudal peduncle). Total lengths were estimated based on regressions between caudal lengths and total lengths from the sampled fish (Table 2).

Fig. 2. Three-dimensional representation of a fish body or swimbladder with 1-mm cylinders (slabs) used in Kirchhoff-ray mode backscatter models.

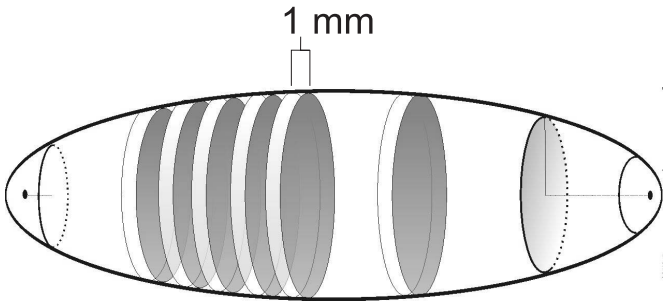

Results

Nine fish groups were modeled. Each group consisted of at least 10 individuals of similar length. The average estimated dorsal swimbladder area varied from 6.4% to 11.3% of the total dorsal body area. Swimbladder volume varied from 2.6% to 3.7% of the total fish volume (Table 3). Capelin had the lowest values in both cases. This species also had the smallest swimbladder angle (mean of 3.9°) and the lowest swimbladder elongation (with corresponding eccentricity).

The effect of length on the mean target strength ($\overline{TS}$) of each species is illustrated at four different frequencies: 12, 38, 120, and 200 kHz (Fig. 3). Among fish of similar lengths, species with a swimbladder had much larger $\overline{TS}$ than species without a swimbladder (differences of up to 15 dB). Differences were also observed among the $\overline{TS}$ of any given species at various carrier frequencies. For example, the $\overline{TS}$ of Pacific herring (Fig. 3*b*) at 12 kHz was consistently 5–10 dB higher than the $\overline{TS}$ at 120 or 200 kHz. Intercepts, shapes, and slopes of the TS to length regressions were also dependent on frequency. At 12 kHz, the increase in $\overline{TS}$ with length was steep and relatively constant. At higher frequencies, successive $\overline{TS}$ peaks and troughs were observed with increasing length. This variability in the $\overline{TS}$ to L_T relationship was particularly marked in species without swimbladders. For example, the $\overline{TS}$ of eulachon peaks and dips twice, spanning more than 10 dB over a 20-cm length range. Variability in TS is attributed to constructive and destructive interference of reflected pressure waves within the fish body.

Intraspecific TS variability was high for species without swimbladders (as illustrated by the standard deviations in Fig. 4). Walleye pollock, a species with a swimbladder, also had high intraspecific TS variability at lengths greater than 40 cm. Capelin and Pacific herring had the smallest range in fish size and intraspecific TS variability. TS of fish modeled at their actual size often differed from the $\overline{TS}$ curve obtained by scaling the lengths of all fish (Fig. 4).

Frequency-dependent backscatter at a specified length and tilt are shown (Fig. 5). Pacific herring and walleye pollock $\overline{TS}$ values were higher at low frequencies, peaking at approximately 20 kHz. The $\overline{TS}$ of these species dropped sharply between 20 and 100 kHz and was relatively constant in the higher frequency range. This sharp decrease in $\overline{TS}$ was not observed for capelin, which exhibited more irregular patterns at lower frequencies. Echo-intensity variance of all fish with swimbladders dramatically increased between 12 and 100 kHz and remained relatively high thereafter. For species without swimbladders, $\overline{TS}$ and standard deviation were highly variable across all frequencies.

Effects of orientation on TS among species with swimbladders were pronounced at high frequencies (Fig. 6). At 12 kHz, the $\overline{TS}$ of a 16-cm capelin or walleye pollock varied by less than 6 dB over a tilt-angle range of 45° to 135°. Pacific herring $\overline{TS}$ decreased by more than 10 dB with increasing tilt angle, but the changes were relatively gradual. In contrast, the $\overline{TS}$ of fish with swimbladders changed sharply with tilt angle at 120 and 200 kHz, especially with orientations approaching swimbladder dorsal incidence (sagittal axis perpendicular to the wave front). Changes in amplitude with orientation were also important at 38 kHz, but the sharp decreases in $\overline{TS}$ occurred at greater tilt angles. It is also noteworthy that the maximum TS for these species with swimbladders did not occur exactly at normal aspect, but at a lower head-down tilt angle (between 80° and 90°). The $\overline{TS}$ of 16-cm Atka mackerel and eulachon varied by more than 30 dB over the range of the tilt angles modeled. The overall pattern (or shape) of the TS – tilt angle relationship for these species without swimbladders was not affected by frequency. At 38 kHz, TS of these fish displayed more variation over small tilt-angle ranges than at 200 or 12 kHz. Changes in $\overline{TS}$ with tilt angle are not symmetrical and depend on the orientation of the individual relative to the wave front (head-down versus head-up) (Fig. 6).

In most cases, TS_θ values were lower than the TS for the same individuals modeled at a 90° tilt (Fig. 4). Differences between these two values were highest for capelin and

Table 1. Acoustic parameters used in Kirchhoff-ray mode models.

Parameter	Freshwater	Marine
Speed of sound in water ($m \cdot s^{-1}$)	1430	1470
Speed of sound in fish body ($m \cdot s^{-1}$)	1570	1570
Speed of sound in swimbladder ($m \cdot s^{-1}$)	—	335
Density of water ($kg \cdot m^{-3}$)	1000	1026
Density of fish body ($kg \cdot m^{-3}$)	1070	1070
Density of swimbladder ($kg \cdot m^{-3}$)	—	7.44

Note: Parameters for the fish body were taken from Clay and Horne (1994). Density of gas within the swimbladder was modeled at a depth of 50 m (607.95 $kN \cdot m^{-2}$).

Table 2. Tilt-angle distribution used for the TS_θ–L_T regressions and equations used to estimate fish total length from the modeled caudal length results (all $r^2 > 0.9$).

Species	Total length	Tilt-angle distribution (mean, SD)
Capelin	1.12CL + 1.43	(93.3, 18.4)[1]
Pacific herring	1.06CL + 0.55	(86.9, 14.2)[2]
Walleye pollock	1.06CL + 1.98	(85.6, 16.2)[3]
Atka mackerel	1.14CL + 0.88	(90, 15)[4]
Eulachon	1.08CL	(90, 15)[4]

Note: [1] Carscadden and Miller (1980); [2] Ona (2001), measurements on Atlantic herring ; [3] Olsen (1971), measurements on Atlantic cod (a related gadoid); [4] conservative values (no published data). CL, caudal length; SD, standard deviation.

Table 3. Mean and standard deviation (in parentheses) for morphological characteristics of the five fish species used in the Kirchhoff-ray mode (KRM) modeling.

Species	*n*	L_T (cm)	L_{KRM}	Sb area (cm^2)	Sb volume (mL)	Area %	Volume %	Sb angle	Body *x*/*y*	Body *e*	Sb *x*/*y*	Sb *e*
Capelin	34	14.2 (1.2)	10–20	1.5 (0.5)	0.3 (0.1)	6.4 (1.3)	2.6 (0.7)	3.9 (2.0)	7.1 (1.1)	0.99	3.9 (0.6)	0.96
Pacific herring	30	23.7 (1.7)	10–30	12.8 (2.5)	6.7 (2.2)	11.3 (1.4)	3.6 (0.8)	7.8 (1.0)	4.1 (0.2)	0.97	5.3 (0.5)	0.98
Walleye pollock	15	15.4 (1.2)	10–20	3.0 (0.8)	0.9 (0.4)	8.4 (0.9)	2.7 (0.6)	6.7 (3.0)	4.9 (0.2)	0.98	4.9 (0.7)	0.98
	10	27.4 (2.5)	20–35	9.6 (1.9)	4.8 (1.2)	9.0 (1.3)	3.0 (0.8)	6.5 (2.3)	5.0 (0.4)	0.98	5.4 (0.7)	0.98
	25	45.1 (4.7)	35–60	39.0 (6.8)	42.9 (12.1)	10.9 (1.3)	3.7 (0.7)	8.5 (2.7)	4.1 (0.4)	0.97	4.3 (0.7)	0.97
Atka mackerel	10	20.5 (2.0)	10–30	—	—	—	—	—	4.1 (1.0)	0.97	—	—
	10	47.4 (3.0)	30–50	—	—	—	—	—	4.6 (0.4)	0.98	—	—
Eulachon	30	17.9 (2.0)	10–20	—	—	—	—	—	5.8 (0.8)	0.98	—	—
	13	24.8 (1.5)	20–30	—	—	—	—	—	5.4 (0.2)	0.98	—	—

Note: All lengths are in centimetres. L_T, the mean total length of the collected specimens; L_{KRM}, the (caudal) length range used in the model; Sb, swimbladder, swimbladder areas were measured in the dorsal plane; Area % and Volume %, the proportion of the swimbladder area or volume to fish body area or volume; Sb angle, the angle of the swimbladder major axis relative to the sagittal axis of the fish body (positive values indicate that the anterior of the swimbladder is above the sagittal axis); *x*/*y*, ratio of major to minor axes as measured on the lateral traces; *e*, eccentricity for corresponding ellipse.

eulachon. The parameters of the TS_θ–L_T regressions obtained from the KRM model results are listed for all species at the five frequencies (*f*) most commonly used in fisheries acoustics (Table 4). The goodness of fit of the TS_θ–L_T relationships was often poor due to high variability in backscatter response. Values of the slope in the log-linear model often differed from 20, and the use of a 20log regression (forced slope) had, in some cases, considerable effect on the resulting goodness of fit (r^2). For fish with swimbladders, the b_{20} values generally decreased with increasing frequency. Capelin had the lowest b_{20} values, followed by walleye pollock and Pacific herring. Walleye pollock had the best-fit regressions (all $r^2 > 0.9$) and the closest agreement between the log-linear and forced-slope (20log) models for the five tested frequencies, with the exception of Atka mackerel at 120 kHz. As expected, the intercepts of the 20log regressions were much lower for fish without swimbladders. Atka mackerel and eulachon had similar b_{20} values. The estimated regression intercepts of eulachon modeled in freshwater were 2–4 dB lower than those modeled in marine conditions.

Discussion

Agreement between KRM model predictions and published TS values was species-dependent. Values obtained from our model on capelin TS were much higher (4–5 dB for the tilt-averaged TS) than in other studies (O'Driscoll and Rose 2001; Jørgensen and Olsen 2002). Reasons for these differences are not clear. Jørgensen (2003) noted differences in the TS of capelin according to condition factor (based on weight–length relationships) and swimbladder length. TS predictions for Pacific herring are in good agreement with documented TS values for this species in fall ($TS = 20\log L_T - 66$ at 120 kHz; Thomas et al. 2002). However, herring used in our study were collected from large spawning aggregations during March 2002 (Sitka Bay, Alaska). Thomas et al. (2002) found that during spring, the b_{20} was 3.2 dB lower than during the fall. Because individuals used for the x-ray imaging were not sacrificed, it was impossible to determine if they had spawned. Herring gonad may modify the shape and size of the swimbladder and increase TS resulting from lipid content. Such characteristics would change once eggs or milt are released from the body cavity. Ona et al. (2001) noted that seasonal variation in the TS of a closely related herring species (*Clupea harengus*) could be as high as 4–8 dB and incorporated a gonadosomatic index (GSI) to improve the TS–length relationship for this species. In situ TS values obtained on stocks of Atlantic herring are typically 4–6 dB lower than our estimates for Pacific herring (Halldorsson and Reynisson 1983; Misund and Øvredal 1988; Rudstam et al. 1988). Walleye pollock TS–length predictions were comparable with documented TS values at 38 kHz (Traynor and Williamson 1983; Foote and Traynor 1988; Traynor 1996). Our estimated b_{20} intercept value was 1.2 dB lower than in the equation currently used for the conversion of acoustic size to fish length in annual surveys in the Gulf of Alaska and the Bering Sea (Foote and Traynor 1988; Guttormsen et al. 2001). Using ex situ measurements of walleye pollock and deformed cylinder models, Sawada et al. (1999) also found predicted TS values 1–3 dB lower than the Foote and Traynor (1988) equation. To our knowledge,

Fig. 3. Mean target strength ($\overline{TS}$) as a function of fish total length for (*a*) capelin (*Mallotus villosus*), (*b*) Pacific herring (*Clupea pallasii*), (*c*) walleye pollock (*Theragra chalcogramma*), (*d*) Atka mackerel (*Pleurogrammus monopterygius*), and (*e*) eulachon (*Thaleichthys pacificus*). Dotted line, 12 kHz; bold unbroken line, 38 kHz; thin unbroken line, 120 kHz; shaded line, 200 kHz. Averaging was done in the linear domain before logarithmic transformation.

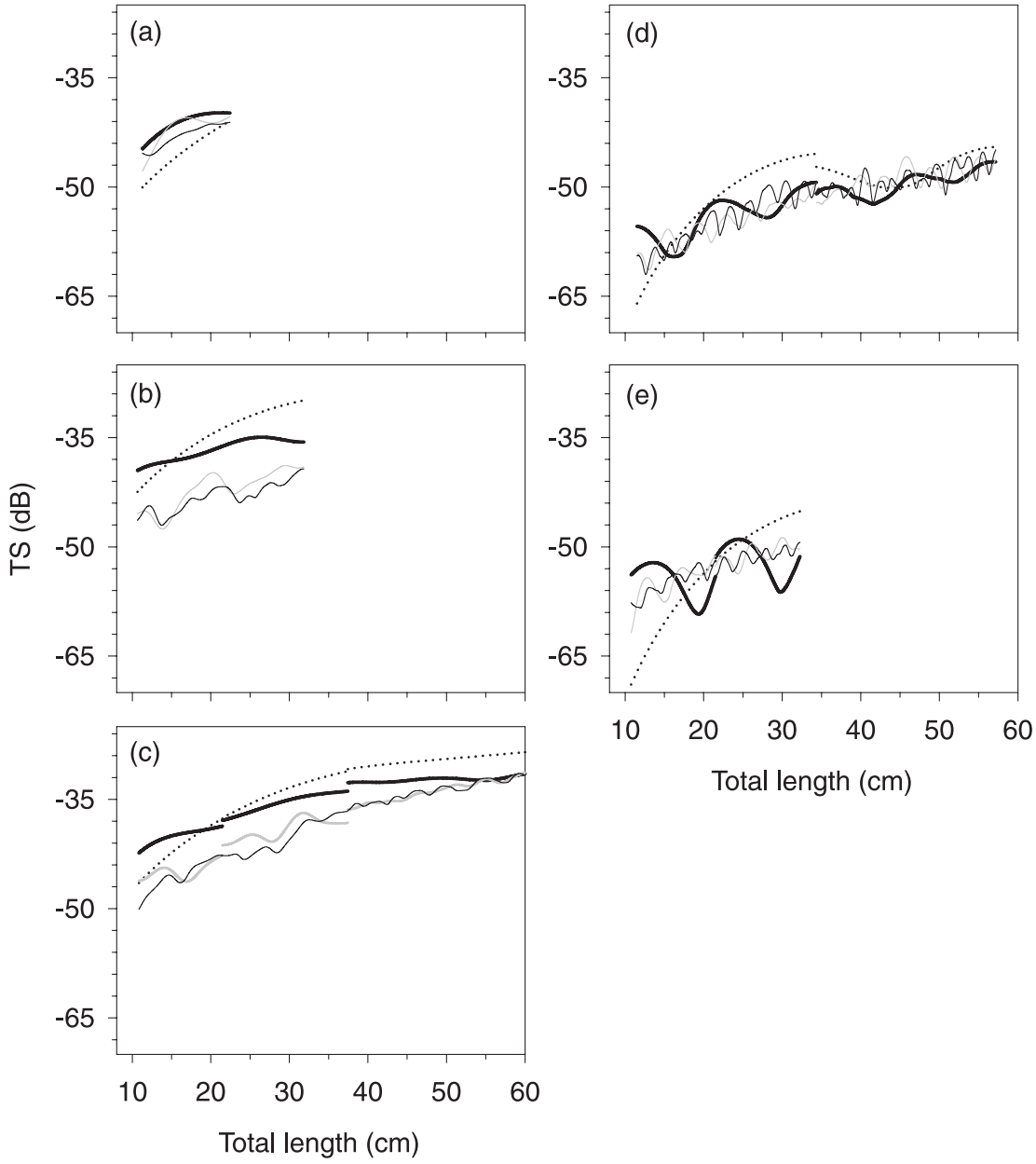

no published data exist on target strengths of Atka mackerel. Experiments on encaged mackerel (*Scomber scombus*) in the Atlantic suggest a b_{20} 1.7–5.7 dB lower (Edwards et al. 1984) than those found in our study. TS estimates for eulachon modeled in marine conditions were similar to those obtained for Atka mackerel of the same length. Predicted eulachon TS from KRM tilt-averaged models adjusted for freshwater were similar to in situ TS measurements of eulachon at 123 kHz (tilt-averaged model = –54.5 dB; mean in situ = –53.5 dB; mean fork length = 18.1 cm) and 208 kHz (tilt-averaged model = –54.9 dB; mean in situ = –50.3 dB; mean fork length = 17.1 cm) in the lower Fraser River, British Columbia (B. Stables, Shuksan Fisheries Consulting, P.O. Box 485, Sumas, WA 98295, USA, personal communication). Even though the 4.6 dB difference at 208 kHz appears large, predicted eulachon backscatter can differ by up to 4 dB within a 1-cm change in length.

Because of the large density and sound speed contrasts of gas and water, the echo intensity of a fish primarily depends on the presence or absence of a gas-filled swimbladder (Haslett 1962; Foote 1980*a*). Contributions of fish flesh and other organs to the total backscatter of a fish are minimal compared with the contributions from the swimbladder. Density and sound speed within the swimbladder will change with gas composition, depth, and temperature. Air is highly compressible compared with water and fish flesh. Its

Fig. 4. Target strength (TS) at 38 kHz as a function of fish total length (L_T) for (*a*) capelin (*Mallotus villosus*), (*b*) Pacific herring (*Clupea pallasii*), (*c*) walleye pollock (*Theragra chalcogramma*), (*d*) Atka mackerel (*Pleurogrammus monopterygius*), and (*e*) eulachon (*Thaleichthys pacificus*). Shaded lines, mean and standard deviation of all fish modeled over a range of scaled length and a tilt angle of 90° (normal aspect); ●, TS of individuals modeled at their default length and a tilt angle of 90°; △, TS of individuals modeled at their default length and averaged over a normal distribution of tilt angles; unbroken line, best fit log-linear regression for TS_θ ($TS_\theta = a\log(L_T) + b_0$); dotted line, best-fit 20log regression for the TS_θ ($TS_\theta = 20\log(L_T) + b_{20}$).

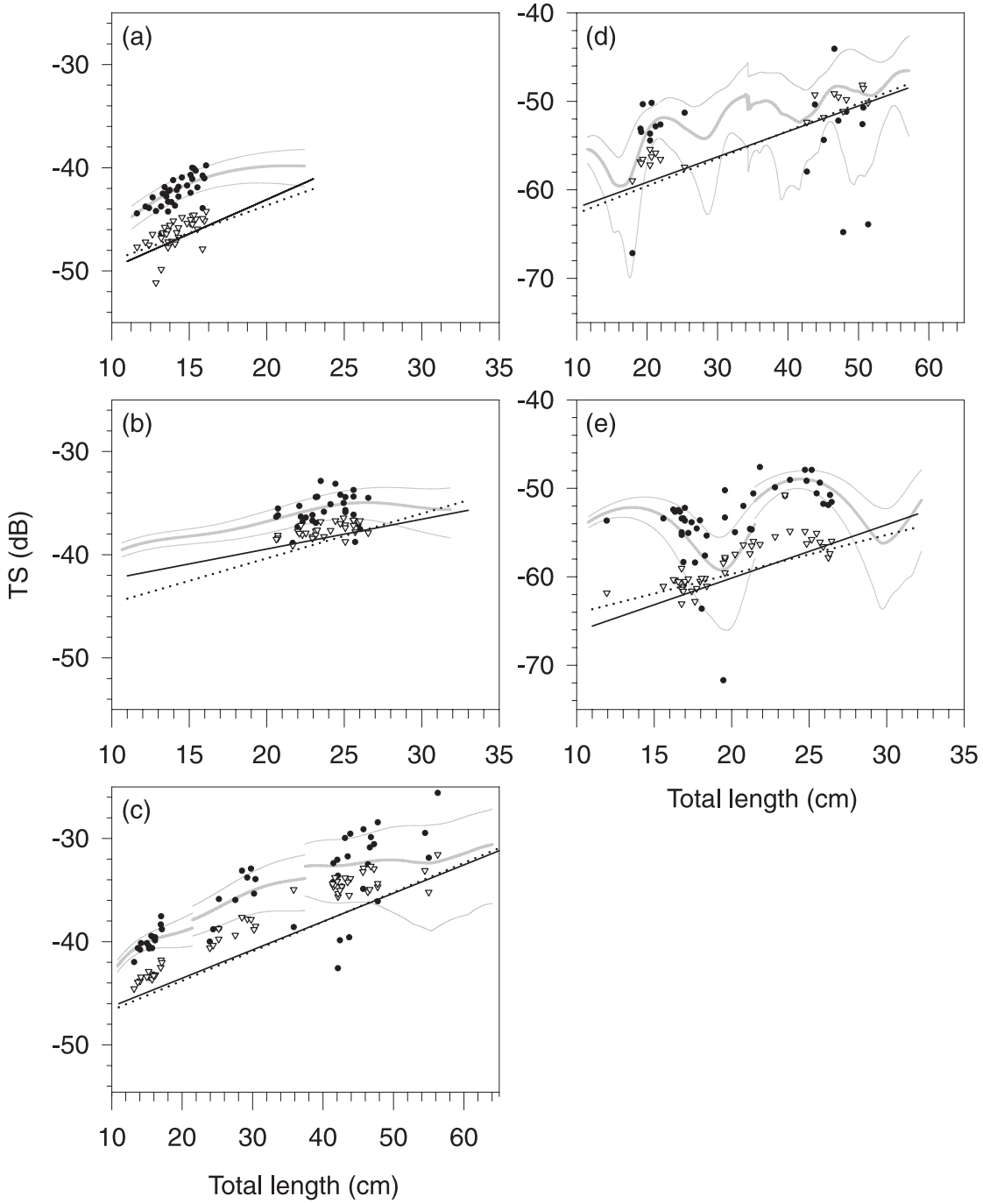

density increases proportionally to pressure (air density = 122.76 kg·m^{-3} at 1000 m). Changes in swimbladder volume as fish change depth according to Boyle's law can have a much more drastic effect on resulting backscatter intensity than density of sound speed contrasts (e.g., Mukai and Iida 1996; Gorska and Ona 2003). Changes in density and sound speed of water also influence KRM model predictions. As an example, TS of eulachon in freshwater were on average 3–4 dB higher than in seawater. Density and sound speed of water are easily calculated using ambient temperature, salinity, and depth (e.g., Mackenzie 1981; UNESCO 1983). Density and sound speed contrasts at interfaces will greatly affect the acoustic scattering of non-gas-bearing organisms (Stanton et al. 2000). Density and sound speeds of fish flesh

Fig. 5. Mean target strength ($\overline{TS}$, bounded by the standard deviation) as a function of frequency for fish scaled to 16 cm: (*a*) capelin (*Mallotus villosus*), (*b*) Pacific herring (*Clupea pallasii*), (*c*) walleye pollock (*Theragra chalcogramma*), (*d*) Atka mackerel (*Pleurogrammus monopterygius*), and (*e*) eulachon (*Thaleichthys pacificus*).

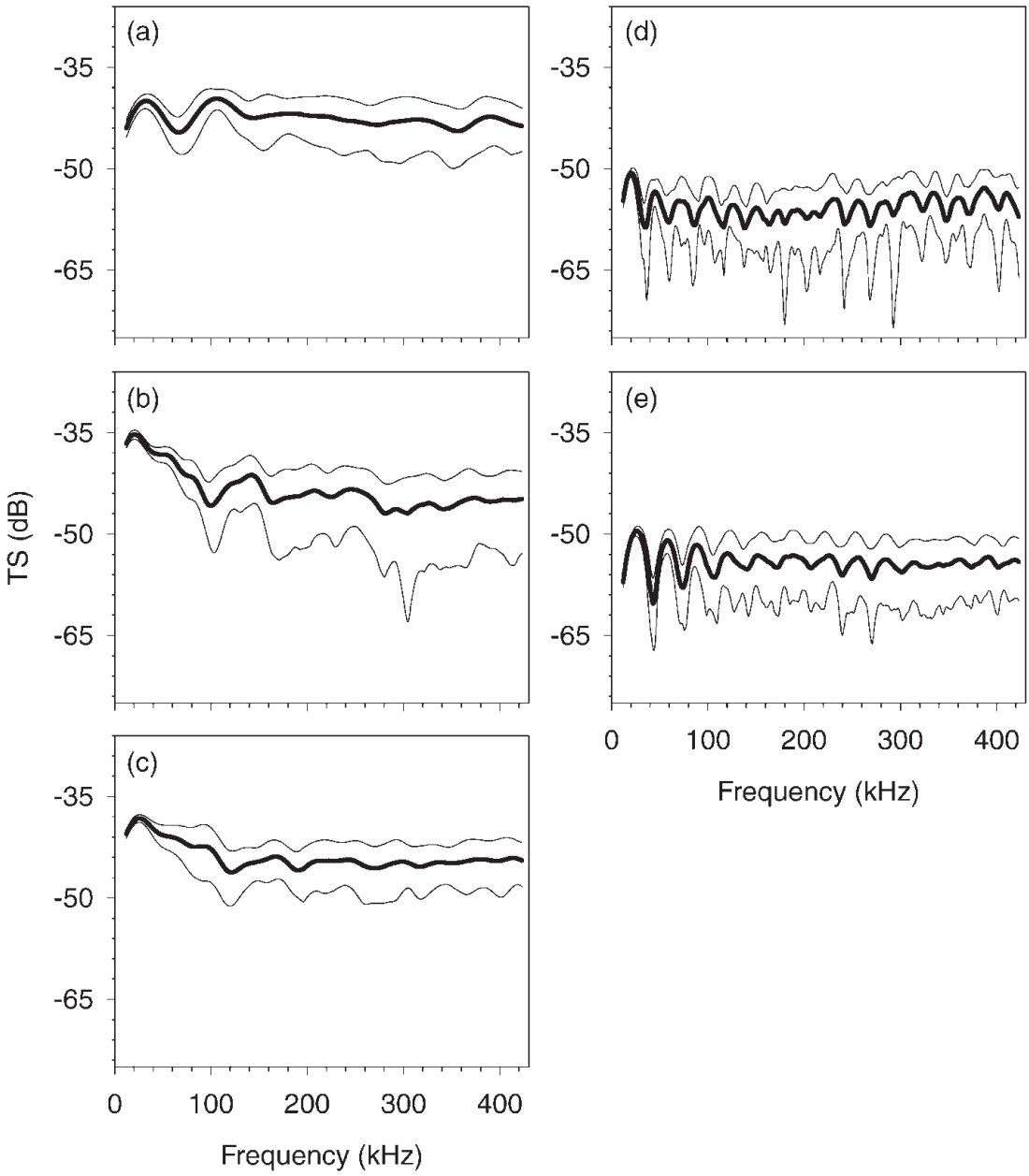

have been documented for a limited number of species (Qiu et al. 1999; McClatchie and Ye 2000; Barr 2001). Changing the sound speed (1548–1570 $m \cdot s^{-1}$) and density (1030–1070 $kg \cdot m^{-3}$) of fish flesh for eulachon and Atka mackerel altered the intercept values from the regressions by as much as 10 dB, but generally not the slopes or shapes of the curves (Gauthier and Horne, unpublished data).

TS of a species depends on several factors that potentially interact. These include the shape and length of the fish, the orientation (i.e., tilt, roll), and the insonyfing frequency. Morphometric (i.e., shape) differences within a species result in variable TS from fish of the same length, especially for species without swimbladders. The extent of this variability, as well as the effects of length on TS, depends on frequency. At 12 kHz, the increase in TS with increasing fish length was relatively constant. At higher frequencies, interactions of the wavelength within the fish body created more constructive and destructive interference. This typically results in more variable TS responses with increasing fish length. The effect of orientation on TS also depends on the presence or absence of a swimbladder and frequency. At 12 kHz, tilt angle has little effect on the TS of fish with swimbladders because of the small ratio of swimbladder length to acoustic wavelength. At any single frequency, the effects are more pronounced as fish size and corresponding swimbladder size increases. Maximum TS occurs at a tilt an-

Fig. 6. Mean target strength ($\overline{TS}$) as a function of fish tilt angle for fish scaled to 16 cm: (*a*) capelin (*Mallotus villosus*), (*b*) Pacific herring (*Clupea pallasii*), (*c*) walleye pollock (*Theragra chalcogramma*), (*d*) Atka mackerel (*Pleurogrammus monopterygius*), and (*e*) eulachon (*Thaleichthys pacificus*). Bold line, 12 kHz; thin line, 38 kHz; shaded line, 200 kHz. Values at 120 kHz were similar to those at 200 kHz and are not plotted.

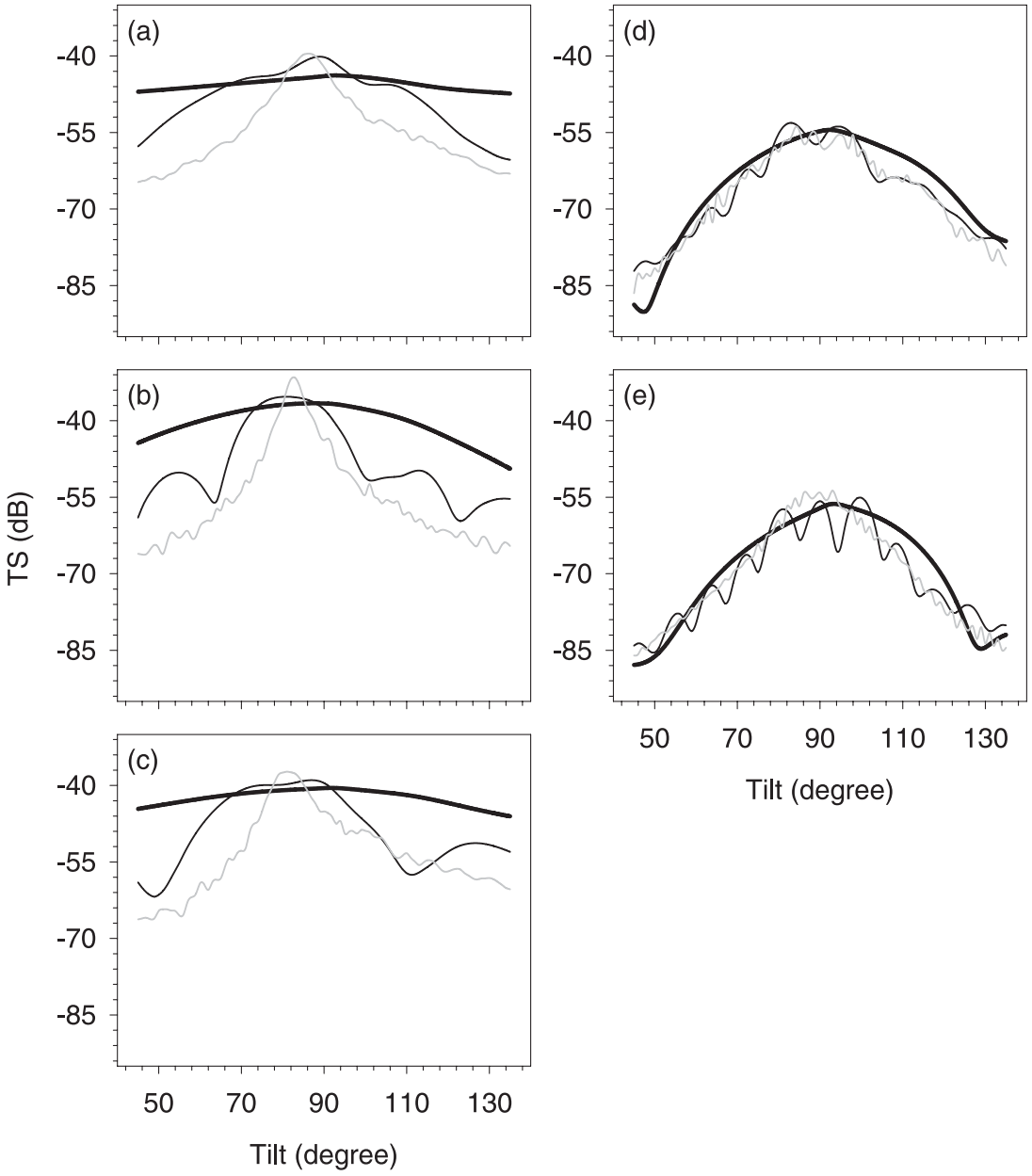

gle lower than normal aspect because of the angle of the swimbladder within the body. The swimbladder in teleost fish typically angles 5° to 10° posterior (Horne and Clay 1998). As the fish body is tilted downward, the swimbladder reaches normal aspect, maximizing the area exposed to the incident wave front. At high frequency (200 kHz), TS decreased sharply as tilt angle deviated from this maxima. Capelin had the lowest swimbladder elongation (and corresponding eccentricity) and showed the least TS variation with tilt angle at any frequency. Capelin also had the lowest proportional swimbladder volume and dorsal area. For species without swimbladders, maximum TS occurred at 90° and decreased gradually. Tilt–TS functions for these species were not as affected by frequency as fish with swimbladders. TS was more sensitive to small changes in tilt angle at higher frequencies.

We used tilt-averaged TS for the TS–length regressions to represent natural variations of tilt angles within fish populations. Among species with swimbladders, the largest difference between TS at normal incidence (90°) and tilt-averaged TS was observed for capelin. This was a surprising result as capelin TS were least affected by tilt angle. The standard deviation of the tilt distribution was higher than that of Pacific herring or walleye pollock. The average tilt angle was head-up for capelin (Carscadden and Miller 1980) versus the head-down orientation for Pacific herring and walleye

Table 4. Slope and intercept regression parameters for tilt-averaged target strength (TS_θ) based on total length (L_T) at five frequencies (f) based on the Kirchhoff-ray mode predictions.

Species	f (kHz)	Slope (a)	b_a	r^2	b_{20}	r^2
Capelin	12	40.0	–93.7	0.54	–70.8	0.41
	38	24.9	–75.0	0.35	–69.3	0.36
	70	11.1	–61.2	0.12	–71.3	0.05
	120	28.4	–81.8	0.62	–72.2	0.57
	200	22.3	–75.9	0.51	–73.2	0.52
Pacific herring	12	21.2	–64.1	0.01	–62.4	0.04
	38	13.3	–55.9	0.34	–65.1	0.27
	70	19.5	–66.1	0.35	–66.8	0.37
	120	21.0	–69.0	0.29	–67.6	0.31
	200	24.2	–74.3	0.32	–68.5	0.33
Walleye pollock	12	21.7	–68.1	0.96	–65.5	0.96
	38	19.2	–66.0	0.96	–67.2	0.96
	70	20.0	–68.2	0.96	–68.2	0.96
	120	21.1	–70.5	0.95	–68.9	0.94
	200	22.5	–73.1	0.96	–69.4	0.95
Atka mackerel	12	17.9	–79.1	0.86	–82.3	0.85
	38	18.5	–81.0	0.91	–83.2	0.91
	70	22.6	–87.6	0.92	–83.7	0.91
	120	19.9	–83.4	0.97	–83.6	0.97
	200	19.6	–83.1	0.93	–83.6	0.93
Eulachon						
Marine	12	40.3	–109.7	0.90	–83.4	0.68
	38	27.3	–94.0	0.66	–84.5	0.62
	70	25.0	–90.9	0.79	–84.4	0.76
	120	15.3	–77.6	0.51	–83.7	0.47
	200	21.5	–86.0	0.80	–84.0	0.80
Freshwater	12	39.8	–104.6	0.92	–80.1	0.70
	38	26.5	–89.5	0.74	–81.1	0.70
	70	23.5	–85.6	0.78	–81.1	0.77
	120	15.0	–73.8	0.61	–80.3	0.55
	200	20.5	–81.3	0.84	–80.7	0.84

pollock. The swimbladder angle for capelin was closer to horizontal, and the response of TS to tilt had a sharper peak at 38 kHz. The combination of tilt range, fish orientation, and tilt-dependent backscatter resulted in lower tilt-averaged TS for capelin than for the other species with swimbladders.

It is noteworthy that the log-linear regressions for walleye pollock and Atka mackerel had slopes near 20. Slopes of TS_θ–L_T regressions often differed from 20 for other species, especially capelin and eulachon. Given the relatively small length range available for these species, it is difficult to ascertain definitive values for the regression parameters. The large differences in goodness of fit (r^2) observed between the log-linear and 20log models suggest that it may not always be appropriate to express TS results using a 20log regression (cf. McClatchie et al. 1996*b*, 2003). Our modeled data also illustrate that regression parameters depend on frequency (especially for species with swimbladders) and that frequency-dependent scattering may be useful for species discrimination.

From our modeling results, we conclude that backscatter characteristics differ among the five species. As expected, the greatest differences were between fish with and without swimbladders. Variability in TS resulting from morphometric differences was high, especially for species without swimbladders. Tilt angle affected backscatter responses. TS–tilt functions also depended on the presence or absence of a swimbladder and its orientation within the fish body. Effects of fish length and tilt angle on TS were frequency-dependent. The slopes of TS_θ–L_T regressions were in many cases different than 20. Based on these results, the next logical step in this work is to examine potential discriminatory metrics using species-specific acoustic properties. Future efforts should also be directed at comparing model predictions with in situ measurements of monospecific and mixed aggregations of fish.

Acknowledgements

We would like to thank Jason Sweet and Rick Towler for their assistance in the field and with the analyses. Funding for this project was provided by the NMFS Steller Sea Lion Research Initiative (award number NA17FX1407), the North Pacific Universities Marine Mammal Consortium (award number NA16FX2629), the Office of Naval Research (N00014–00–1–0180), and the Alaska Fisheries Science Center (NA17RJ1232-AM01).

References

Alverson, D.L. 1992. A review of commercial fisheries and the Steller sea lion (*Eumetopias jubatus*): the conflict arena. Rev. Aquat. Sci. **6**: 203–256.

Barr, R. 2001. A design study of an acoustic system suitable for differentiating between orange roughy and other New Zealand deep-water species. J. Acoust. Soc. Am. **109**: 164–178.

Blaxter, J.H.S., and Batty, R.S. 1990. Swimbladder "behaviour" and target strength. Rapp. P.-V. Réun. Comm. Int. Explor. Mer, **189**: 233–244.

Carscadden, J.E., and Miller, D.S. 1980. Estimates of tilt angle of capelin using underwater photographs. ICES CM 1980/H:50.

Clay, C.S., and Horne, J.K. 1994. Acoustic models of fish: the Atlantic cod (*Gadus morhua*). J. Acoust. Soc. Am. **96**: 1661–1668.

Edwards, J.I., Armstrong, F., Magurran, A.E., and Pitcher, T.J. 1984. Herring, mackerel, and sprat target strength experiments with behavioral observations. ICES CM 1984/B:34.

Foote, K.G. 1980*a*. Importance of the swimbladder in acoustic scattering fish: a comparison of gadoid and mackerel target strengths. J. Acoust. Soc. Am. **67**: 2084–2089.

Foote, K.G. 1980*b*. Effect of fish behaviour on echo energy: the need for measurements of orientation distributions. J. Cons. Int. Explor. Mer, **39**: 193–201.

Foote, K.G. 1982. Optimizing copper spheres for precision calibration of hydroacoustic equipment. J. Plankton Res. **71**: 742–747.

Foote, K.G., and Francis, D.T.I. 2002. Comparing Kirchhoff-approximation and boundary-element models for computing gadoid target strengths. J. Acoust. Soc. Am. **111**: 1644–1654.

Foote, K.G., and Traynor, J.J. 1988. Comparison of walleye pollock target strength estimates determined from *in situ* measurements and calculations based on swimbladder form. J. Plankton Res. **83**: 9–17.

Gorska, N., and Ona, E. 2003. Modelling the effect of swimbladder compression on the acoustic backscattering from herring at normal or near-normal dorsal incidences. ICES J. Mar. Sci. **60**: 1381–1391.

Guttormsen, M.A., Wilson, C.D., and Stienessen, S. 2001. Echo integration-trawl survey results for walleye pollock in the Gulf of Alaska during 2001. *In* Stock Assessment and Fishery Evaluation Report for the Groundfish Resources of the Gulf of Alaska, November 2001. Prepared by the Gulf of Alaska Groundfish Plan Team, North Pacific Fishery Management Council, P.O. Box 103136, Anchorage, AK 99510.

Halldorsson, O., and Reynisson, P. 1983. Target strength measurement of herring and capelin in-situ at Iceland. FAO Fish. Rep. No. 300.

Haslett, R.W.G. 1962. The back-scattering of acoustic waves in water by an obstacle. II. Determination of the reflectivities of solids using small specimens. Proc. Phys. Soc. Lond. **79**: 559–571.

Horne, J.K. 2003. The influence of ontogeny, physiology, and behaviour on the target strength of walleye pollock (*Theragra chalcogramma*). ICES J. Mar. Sci. **60**: 1063–1074.

Horne, J.K., and Clay, C.S. 1998. Sonar systems and aquatic organisms: matching equipment and model parameters. Can. J. Fish. Aquat. Sci. **55**: 1296–1306.

Horne, J.K., Walline, P.D., and Jech, J.M. 2000. Comparing acoustic model predictions to *in situ* backscatter measurements of fish with dual-chambered swimbladders. J. Fish Biol. **57**: 1105–1121.

Jech, J.M., Schael, D.M., and Clay, C.S. 1995. Application of three sound scattering models to threadfin shad (*Dorosoma petenense*). J. Acoust. Soc. Am. **98**: 2262–2269.

Jørgensen, R. 2003. The effects of swimbladder size, condition and gonads on the acoustic target strength of mature capelin. ICES J. Mar. Sci. **60**: 1056–1062.

Jørgensen, R., and Olsen, K. 2002. Acoustic target strength of capelin measured by single-target tracking in a controlled cage experiment. ICES J. Mar. Sci. **59**: 1081–1085.

Mackenzie, K.V. 1981. Nine-term equation for sound speed in the oceans. J. Acoust. Soc. Am. **70**: 807–812.

McClatchie, S., and Ye, Z. 2000. Target strength of an oily deep-water fish, orange roughy (*Hoplostethus atlanticus*). II. Modeling. J. Acoust. Soc. Am. **197**: 1280–1285.

McClatchie, S., Alsop, J., Ye, Z., and Coombs, R.F. 1996*a*. Consequence of swimbladder model choice and fish orientation to target strength of three New Zealand fish species. ICES J. Mar. Sci. **53**: 847–862.

McClatchie, S., Alsop, J., and Coombs, R.F. 1996*b*. A re-evaluation of relationships between fish size, acoustic frequency, and target strength. ICES J. Mar. Sci. **53**: 780–791.

McClatchie, S., Macaulay, G.J., and Coombs, R.F. 2003. A requiem for the use of $20\log_{10}$length for acoustic target strength with special reference to deep-sea fishes. ICES J. Mar. Sci. **60**: 419–428.

Misund, O.A., and Øvredal, J.T. 1988. Acoustic measurements of schooling herring: estimation of school biomass and target strength. ICES CM 1988/B:26.

Mukai, T., and Iida, K. 1996. Depth dependence of target strength of live kokanee salmon in accordance with Boyle's law. ICES J. Mar. Sci. **53**: 245–248.

Nakken, O., and Olsen, K. 1977. Target strength measurements of fish. Rapp. P.-V. Réun. Comm. Int. Explor. Mer, **170**: 52–69.

O'Driscoll, R.L., and Rose, G.A. 2001. *In situ* acoustic target strength of juvenile capelin. ICES J. Mar. Sci. **58**: 342–345.

Olsen, K. 1971. Orientation measurements of cod in Lofoten obtained from underwater photographs and their relation to target strength. ICES CM 1971/B:17.

Ona, E. 1990. Physiological factors causing natural variations in acoustic target strength of fish. J. Mar. Biol. Assoc. U.K. **70**: 107–127.

Ona, E. 2001. Herring tilt angles measured through target tracking. *In* Herring: expectations for a new millenium. *Edited by* F. Funk, J. Blackburn, D. Hay, A.J. Paul, R. Stephenson, R. Toresen, and D. Witherell. Lowell Wakefield Fisheries Symposia Series, Fairbanks, Alaska. pp. 509–519.

Ona, E., Zhao, X., Svellingen, I., and Fosseidengen, J. E. 2001. Seasonal variation in herring target strength. *In* Herring: expectations for a new millenium. *Edited by* F. Funk, J. Blackburn, D. Hay, A.J. Paul, R. Stephenson, R. Toresen, and D. Witherell. Lowell Wakefield Fisheries Symposia Series, Fairbanks, Alaska. pp. 461–487.

Qiu, X.F., Zhang, R.H., Li, W.H., Jin, G.L., and Zhu, B.X. 1999. Frequency-selective attenuation of sound propagation and reverberation in the Yellow Sea. J. Sound Vib. **220**: 331–342.

Rose, G.A., and Porter, D.R. 1996. Target-strength studies on Atlantic cod (*Gadus morhua*) in Newfoundland waters. ICES J. Mar. Sci. **53**: 259–265.

Rosen, D.A.S., and Trites, A.W. 2000. Pollock and the decline of Steller sea lions: testing the junk-food hypothesis. Can. J. Zool. **78**: 1243–1250.

Rudstam, L.G., Lindem, T., and Hansson, S. 1988. Density and *in situ* target strength of herring and sprat: a comparison between two methods of analyzing single-beam sonar data. Fish. Res. **6**: 305–315.

Sawada, K., Ye, Z., Kieser, R., Mcfarlane, G.A., Miyanohana, Y., and Furusawa, M. 1999. Target strength measurements and modeling of walleye pollock and Pacific hake. Fish. Sci. **65**: 193–205.

Stanton, T.K., Chu, D., Wiebe, P.H., Eastwood, R.L., and Warren, J.D. 2000. Acoustic scattering by benthic and planktonic shelled animals. J. Acoust. Soc. Am. **108**: 535–550.

Stickney, R.R. 2000. Responses of pinniped populations to directed harvest, climate variability, and commercial fishery activity: a comparative analysis. Res. Fish. Sci. **8**: 89–124.

Thomas, G.L., Kirsh, J., and Thorne, R.E. 2002. *Ex situ* target strength measurements of Pacific herring and Pacific sand lance. N. Am. J. Fish. Manag. **22**: 1136–1145.

Traynor, J.J. 1996. Target-strength measurements of walleye pollock (*Theragra chalcogramma*) and Pacific whiting (*Merluccius productus*). ICES J. Mar. Sci. **53**: 253–258.

Traynor, J.J., and Williamson, N.J. 1983. Target strength measurements of walleye pollock (*Theragra chalcogramma*) and a simulation study of the dual beam method. FAO Fish. Rep. No. 300.

Trites, A.W., and Donnelly, P.L. 2003. The decline of Steller sea lions in Alaska: a review of the nutritional stress hypothesis. Mammal Rev. **33**: 3–28.

United Nations Educational, Scientific and Cultural Organization (UNESCO). 1983. Algorithms for computations of fundamental properties of seawater. UNESCO Tech. Pap. Mar. Sci. **44**: 1–53.